Demonstration of the ESL-IIP Radiometer's Asynchronous Pulse Blanker: Mitigation of an Air Traffic Control Radar

Grant Hampson* and Steve Ellingson†

July 26, 2002

1 Introduction

This document presents the results of the first use of the ESL-IIP radiometer's recently-completed asynchronous pulse blanker (APB) subsystem to successfully mitigate pulsed radio frequency interference (RFI) originating from an air traffic control (ATC) radar in real time. This demonstration also marks the first on-the-air use of the FPGA-based Fast Fourier Transform (FFT), which is used here primarily to accelerate the analysis of the data.

2 The ESL-IIP Radiometer

The ESL-IIP radiometer is an experimental system designed to allow airborne high-sensitivity passive L-band remote sensing in the presence of RFI [1]. The current design baseline specifies an instantaneous bandwidth of 100 MHz, in which nearly all processing is done after digitization [2]. The radiometer uses several stages of RFI mitigation to deal with the various forms of interference present in L-band [3]. This report is concerned with the asynchronous pulse blanker (APB) [4], whose function

*The Ohio State University, ElectroScience Laboratory, 1320 Kinnear Road, Columbus, OH 43210, USA. Email: hampson.8@osu.edu.

†The Ohio State University, ElectroScience Laboratory, 1320 Kinnear Road, Columbus, OH 43210, USA. Email: ellingson.1@osu.edu

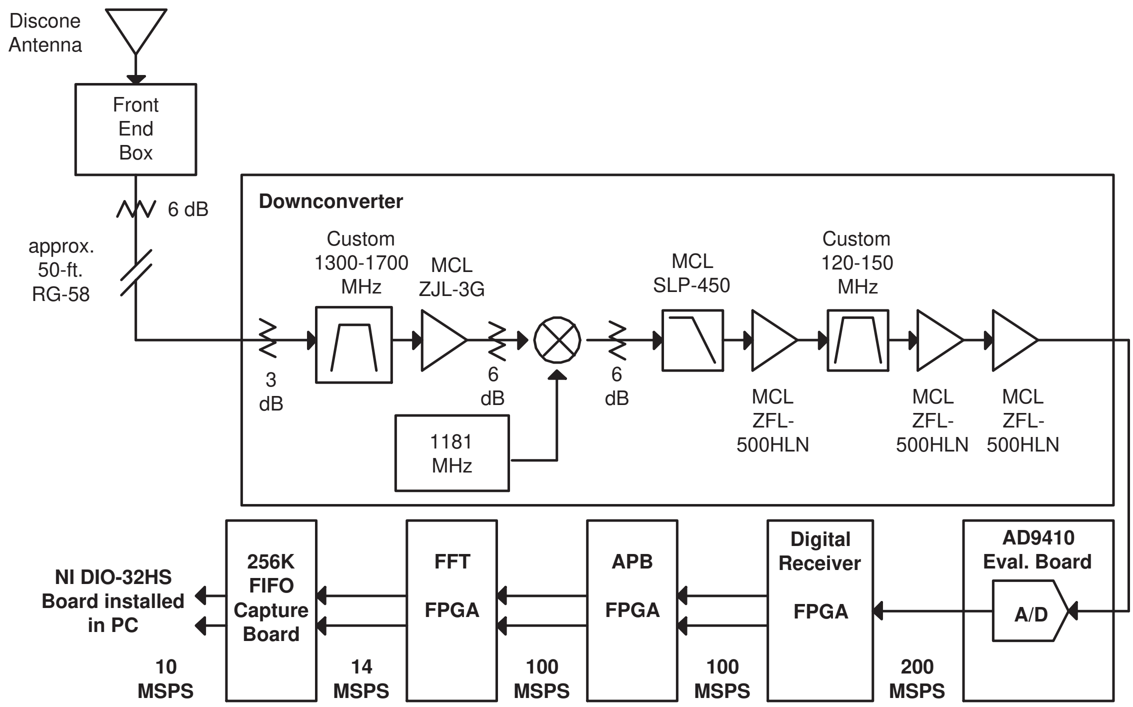

Figure 1: Current ESL-IIP radiometer setup. The antenna and front end box are not part of the system *per se*, but are used here simply to facilitate the experiment.

is to mitigate pulsed interference. In L-band, this form of RFI is normally associated with air traffic control (ATC) radars.

Figure 1 shows a block diagram of the ESL-IIP radiometer as it currently exists. At this point, we emphasize that the radiometer is *not* complete. However, we have been following a modular "test-as-you-go" development strategy which has allowed us to put a minimally-capable system on the air early in the project timeline, and add functionality as the associated hardware is completed.

The discone antenna and "front end box" (a temporary RF front end containing a low noise amplifier and various other components needed near the antenna) are shown in Figure 2 and are identical to those described in [5]. The front end box has about 26 dB gain, 3 dB noise figure, and a 1-dB compression of about −30 dBm at the antenna terminals. The downconverter, shown in Figure 3, is identical to the proposed IIP design [6], except for the following: (1) the analog blanker and digital step attenuator are not yet installed, and (2) due to a problem with the LO synthesizer, the LO level at the mixer is only +2 dBm (+7 dBm is nominal) and there is no matching pad. The output of the downconverter is an IF signal bandlimited to 120 MHz – 180 MHz (60 MHz IF bandwidth). The analog IF is input to the digital processing section shown in Figure 4 and originally described in [7]. The A/D digitizes to 10 bits at 200 MSPS. The digital receiver FPGA does quadrature demodulation, filtering to 50 MHz bandwidth, and decimation to 100 MSPS. (See [7] for details on the A/D + Digital Receiver implementation.) This is followed by successive FPGA stages implementing the APB and an FFT, respectively (more detail on these below). For the purposes of the testing described in this memo, the output is captured using a 256K-sample FIFO described in [8], which also interfaces to a personal computer (PC) via a National Instruments PCI-DIO-32HS card.

The design concept and implementation of the APB are described in [4] and [9], respectively. For the convenience of the reader, we will briefly summarize the essentials here. Under normal conditions, the APB simply delays the data by routing it through a first-in first-out (FIFO) buffer, and computes a running estimate of the mean and variance of the noise. Whenever a sample with magnitude greater than β (typically, $\beta = 10$) standard deviations above the mean is detected at the input to the FIFO, a blanking event is triggered.* At the output of the APB's FIFO, a block of samples are set to zero, starting well before the triggering sample, and concluding well after the triggering sample. A contiguous block of samples is blanked (as opposed to individual samples) to ensure that weak precursor and postcursor multipath components (that may not themselves be strong enough to trigger the blanker) are also eliminated. β and the blanking window parameters are dynamically selectable by the user via an ethernet connection to a tiny "Rabbit" microcontroller, which is mounted mezzanine-fashion on the APB board (see Figure 4). Appropriate values depend on the nature of the RFI being observed. The APB can be disabled and placed in a "pass through" mode to allow comparisons between APB-processed and unprocessed data.

*Note: Sometimes we talk in terms of values of β, and sometimes β^2. Sorry for the inconvenience.

Figure 2: Antenna and front end box, as mounted on the roof of ESL. The antenna is about 10 m above ground level.

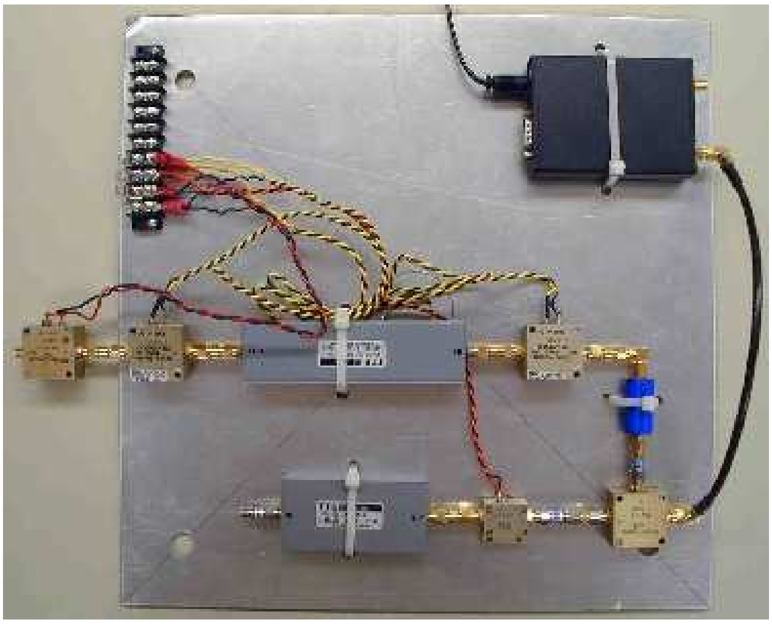

Figure 3: Interim downconverter.

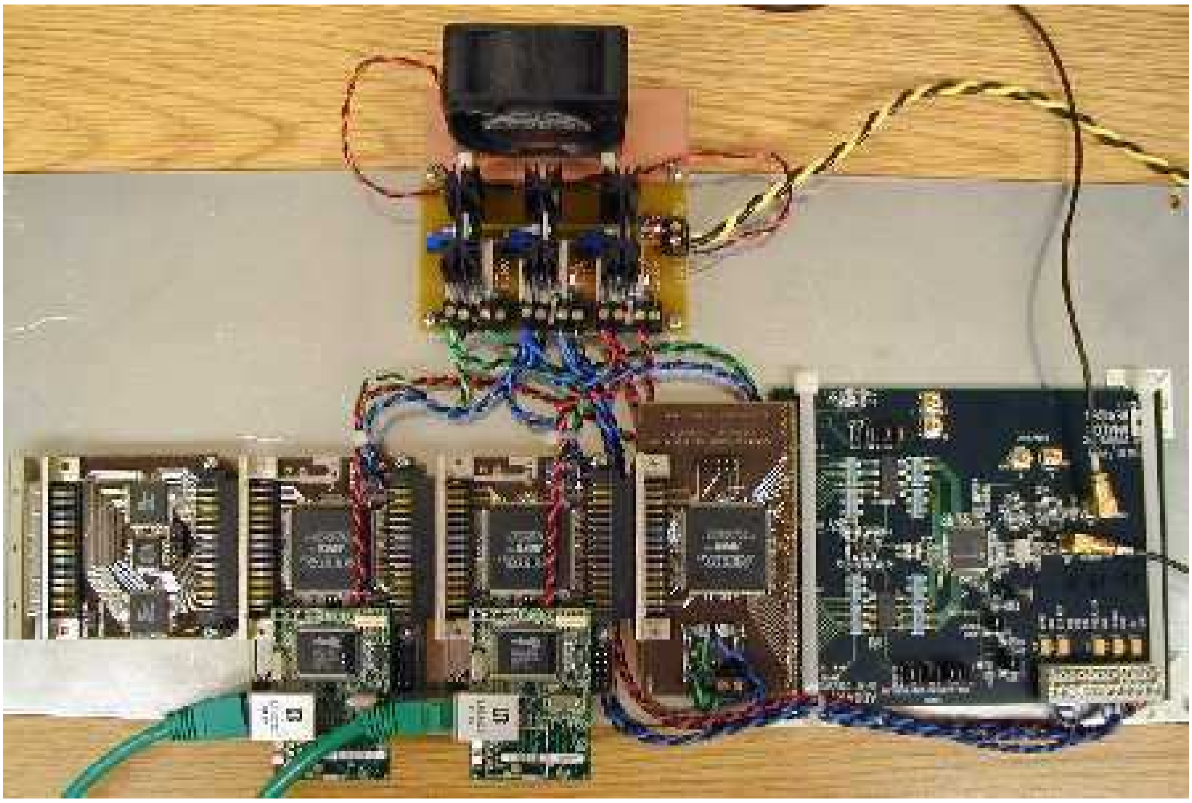

Figure 4: Digital processing section. From right to left: AD9054 A/D, Digital Receiver Board, APB Board, FFT Board, FIFO Capture Board. Center top: Power regulation and distribution. Note also the Rabbit microcontrollers connected to the APB and FFT boards, proving a control path via an ethernet network.

Following the APB is an FFT processor [10], which is used here simply as a means to reduce the computational burden in the post-processing software.† The FFT operates on 1K (1024 samples, or 10.24 μs) complex samples, and the input is not windowed. The FFT throughput is 14 MSPS. 254 1K complex FFT outputs ($\approx$2.6 ms effective, 18.6 ms actual) are captured in the FIFO capture board, and then transferred to the PC at 10 MSPS. Due to the limited throughput of the FFT and capture boards, the effective duty cycle with respect to integration time is upper-bounded at 10% in this experiment; e.g., the effective integration time is 10% of the elapsed time.

A C-language program running on the PC acquires, processes, and saves data. For each set of 254 FFT outputs downloaded from the FIFO capture board, the PC computes the max-hold and averaged spectra. ("Max-hold" spectra are computed by taking the maximum value across all input spectra on a bin-by-bin basis.) This process repeats 100 times, yielding a single max-hold spectrum and a single averaged spectrum representing 260 ms of integration time. This cycle requires 30 s to complete, so the observation duty cycle is about 0.9%, limited primarily by PC processing. (However, we emphasize that the final IIP radiometer will operate 100% duty cycle, enabled by an FFT processor/integrator board currently under development.)

3 The London ATC Radar

The strongest pulsed RFI source received at our location is an ATC radar located in London, OH, approximately 43 km distant. Previous observations of this radar are reported in [5] and [11]. This radar transmits pulses centered at 1331 MHz about 2 μs long every 3 ms, with 3 MW peak transmit power. Most of the spectrum is contained within about 2 MHz, but sidelobes have been detected over a span of at least 6 MHz (as will be shown later). The radar uses an antenna with a very narrow beam that rotates in azimuth at a rate of 0.1 Hz. Thus, the radar is very strong

†The completed radiometer will use the same FFT FPGA core, except eight FFTs will be configured in parallel on a dual-FPGA board to achieve 100 MSPS throughput, and will be followed by bin-blanking and integration functions as described in [3].

for a few milliseconds every 10 s, and is relatively weak otherwise. It is also worth emphasizing that the received signal often contains a complex mix of postcursor and precursor components, representing multipath from terrain and aircraft [11]. Based on the findings of [11], we chose to define a blanking window beginning 5 μs before the triggering sample and ending 35 μs after the triggering sample. Since the pulses from this radar are spaced about 3 ms apart, no more than 1.4% of the available data is expected to be blanked as a result.

4 "Off-Line" Emulation of the APB Using Captured Data

Before testing the APB on the air, we performed a sanity check of our system using a single block of data downloaded from the FIFO capture buffer. The data was collected with both the APB and FFT disabled (i.e., in pass-through mode). This allowed us to capture a block of 256K contiguous complex samples for post-processing analysis. In pass-through mode, the APB continues to operate, but instead of blanking the data, it simply outputs an additional 1-bit signal indicating when it would choose to blank.

Figure 5 shows a single pulse from the radar collected in this manner. Also shown is the APB blanking status signal for $\beta = 10$. As indicated in this figure, 500 precursor samples and 3500 postcursor samples are blanked, resulting in a blanking window of length 40 μs as expected. Using this method of observation, we confirmed that the dynamic range of the receiver was never exceeded as a result of this or any other received signal. In other words, we are confident that the analog sections of the receiver are never close to compression, nor is there any "clipping" of the A/D or subsequent digital processing stages.

As mentioned above, we selected the detection threshold for triggering in this part of the experiment to be $\beta = 10$. This decision is based on previous studies showing this to be a reasonable tradeoff between excessive spurious triggering (β too small)

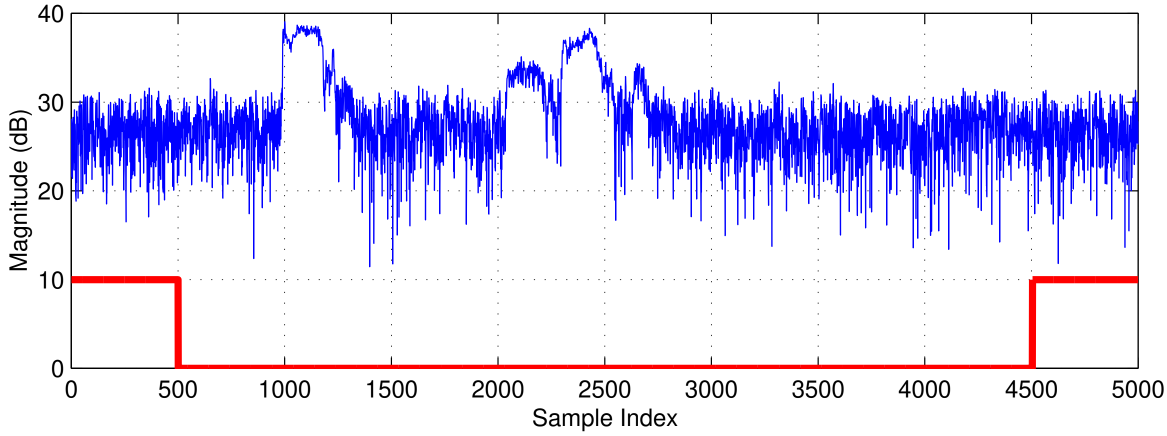

Figure 5: A time series showing a single pulse from the London ATC radar. 5000 samples = 50 μs. The main pulse starts at sample index 1000. At least 3 distinct postcursor multipath components are visible. The selected blanking window is shown in red (this is a binary signal – vertical axis units do not apply to this curve). The APB triggers on sample index 1000.

and passing of weak pulses (β too large) [4, 12]. In Section 5, the effect of varying β will be considered.

Using the captured time series and the APB blanking signal, we then emulated (in software) the procedure followed by the APB, FFT, and capture card as described in Section 2. Since the record length is only about 2.6 ms, we have captured only one pulse event. The results are shown in Figure 6. Two cases are shown: one in which the APB is disabled (in pass-through mode, i.e., "blanking off"), and one in which the APB is enabled (i.e., "blanking on"). Note that the APB procedure effectively removes the radar from the integrated spectrum.

The spurs at +6 MHz and +31 MHz are internally-generated spurious signals. Since these are weak and always present, they are not detected nor acted upon by the pulse blanking procedure.

5 Real-Time APB Demonstration

In this section, we conduct the observations described in Section 2 – including the APB and FFT – and present the results. Figure 7 shows the results for a single cycle of processing (260 ms effective observation time), with the APB enabled and disabled

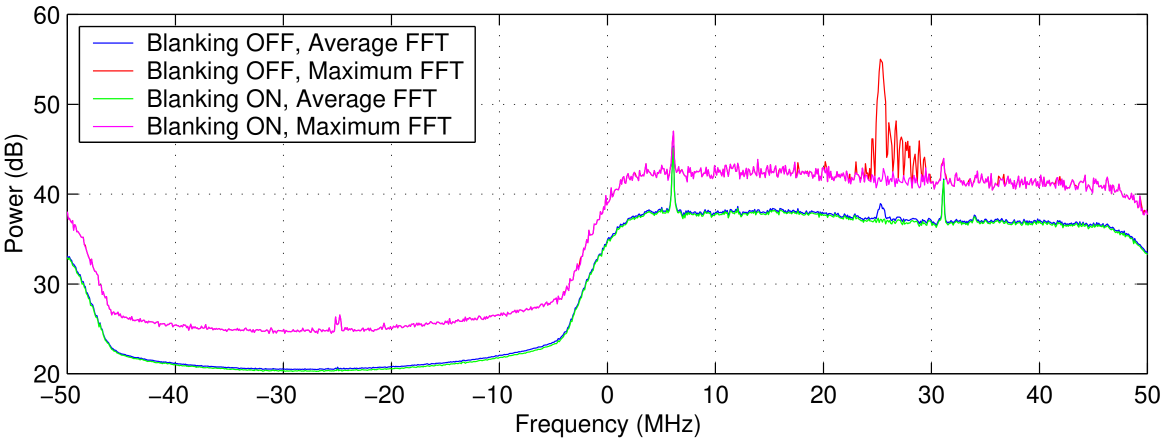

(a) Complete baseband spectrum

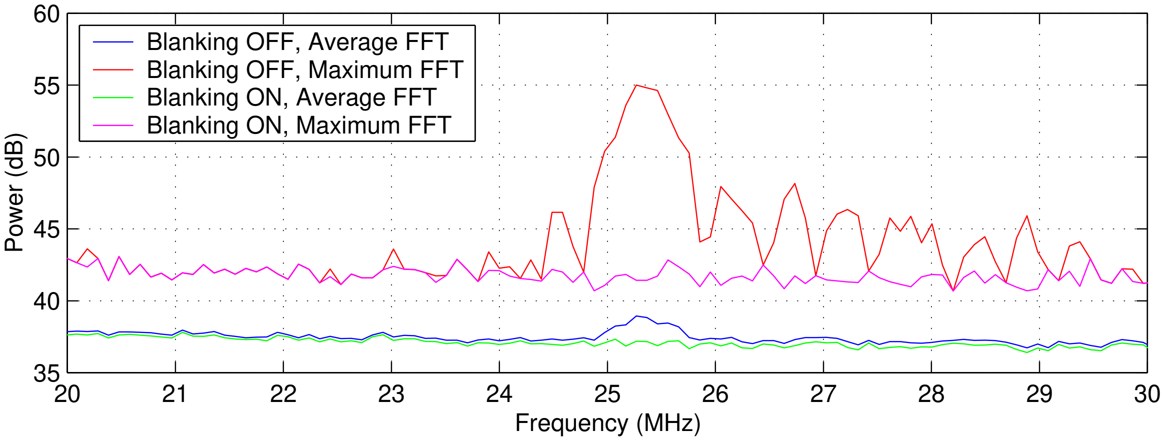

(b) Zooming in on the region of the London ATC radar.

Figure 6: Software emulation of the APB/FFT procedure described in Section 2 using a single contiguous 2.6-ms-long time series. Note: The frequency axis origin corresponds to a received frequency of 1305 MHz. Also, "Maximum FFT" means the same thing as "max-hold", defined earlier.

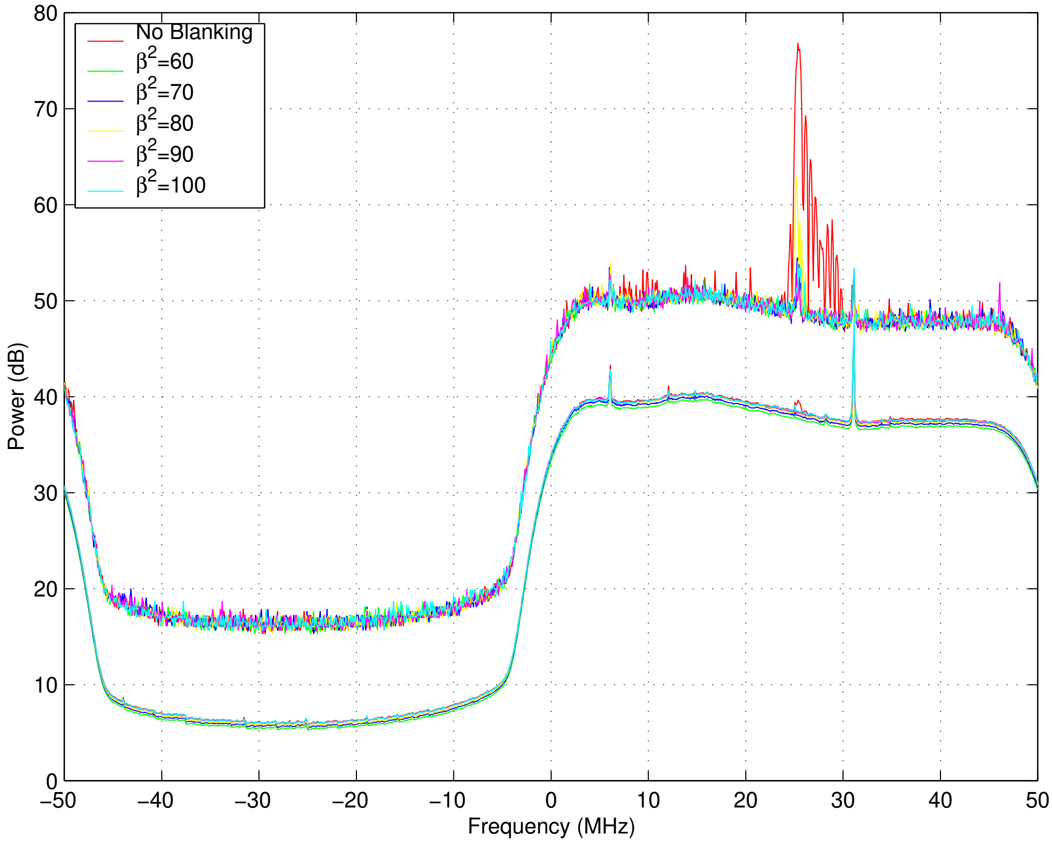

Figure 7: Real-time APB demonstration. Upper cluster of curves are max-hold, lower cluster are average.

(pass-through), for various β. Over this period of time, we expect that about 86 pulse events attributable to the London ATC radar occur, although we cannot say if any of these correspond to illumination by the radar's main beam. It is clear, however, that there is no other in-band RFI with strength comparable to that of the London ATC radar.

Figure 7 indicates that the APB has in fact suppressed the radar. However, interpretation is complicated by the fact that blanking reduces the total power captured during the experiment, which manifests itself as a slight decrease in the mean noise power spectral density (baseline) with decreasing β. However, by monitoring the APB blanking status signal described in Section 4, we can determine the amount of data blanked in each case, and then apply a correction such that the noise spectral baselines are independent of β. This is done in Figure 8. Figure 9 shows the same

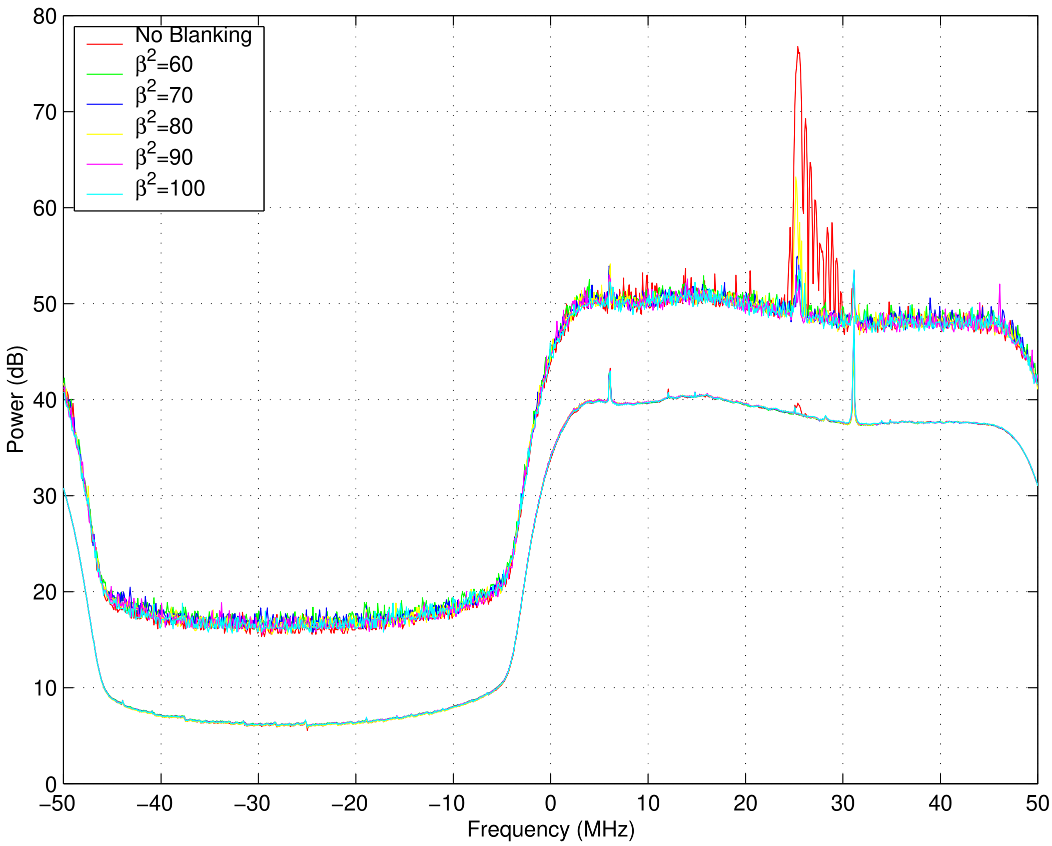

Figure 8: Real-time APB demonstration (normalized baselines). Upper cluster of curves are max-hold, lower cluster are average.

result, now zooming in to the region around the radar. Note that any value of $\beta \leq 10$ greatly suppresses the radar in the integrated spectrum. It is difficult to quantify the suppression, however, since the limited sensitivity of the measurement, combined with the low duty cycle of the radar, results in a diminished effect from the radar even without blanking.

The max-hold results are a little more revealing in this sense. It is interesting to note that the suppression in the max-hold spectra does not seem to increase monotonically with decreasing β, as expected. We speculate that this is due to the tendency of the blanker to trigger on strong noise samples, which may cause it to miss much bigger *bona fide* radar pulses occuring shortly (i.e., on the order of 40 μs) thereafter. It may also be that such spurious triggering is in fact legitimate, and is associated with weak radars that we have not yet identified. A measurement campaign is needed

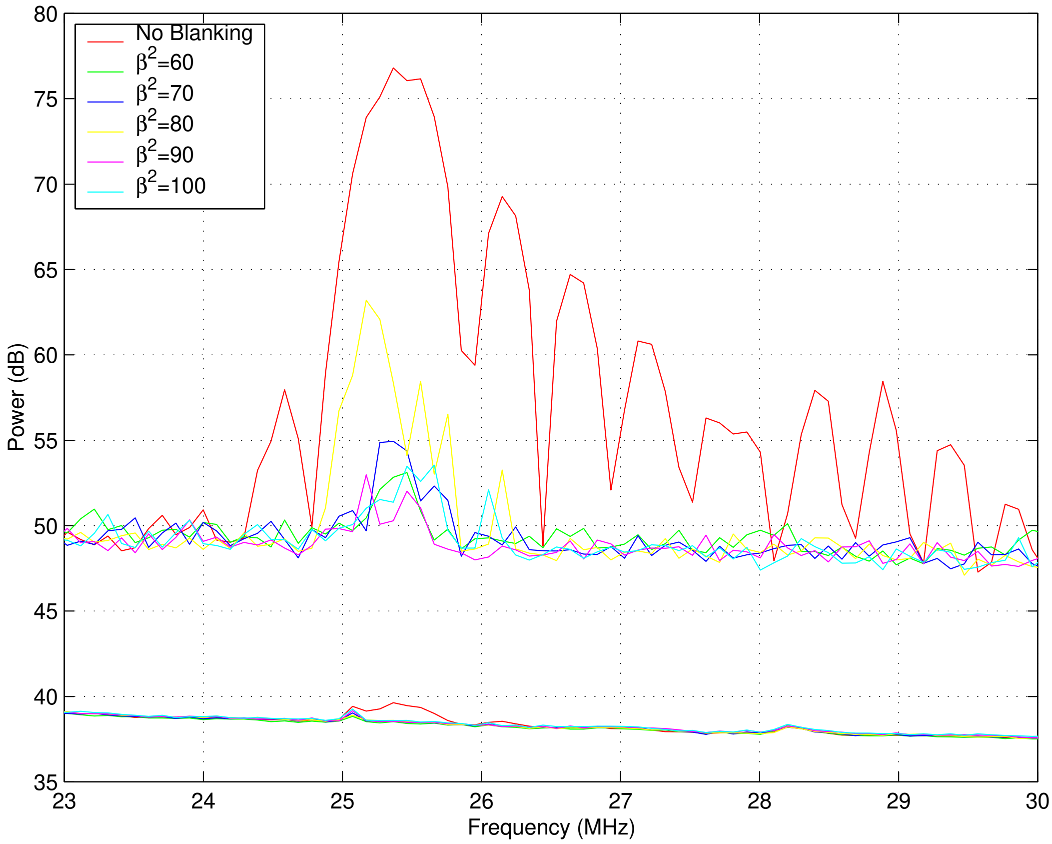

Figure 9: Same as Figure 8, zooming in on region of the ATC radar.

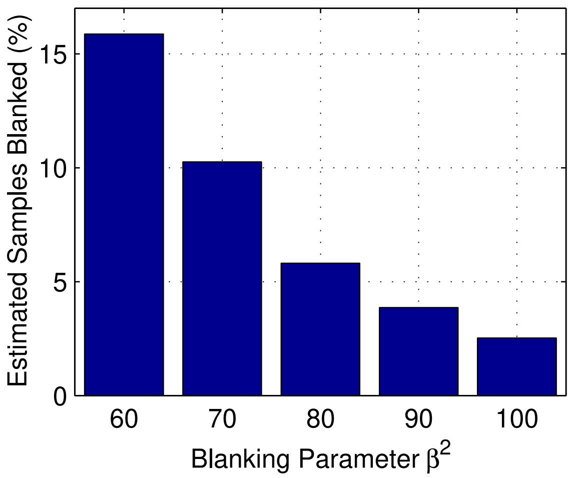

Figure 10: Percentage of samples blanked (estimated from measured change in the spectral baseline) as a function of β.

to better understand this issue. Meanwhile, this does not appear to be a concern since the APB is designed to accommodate at least 4 independently-triggerable, overlapping blanking windows, although only one was used in this experiment. This feature should prevent the problems that occur when multiple pulses arrive within a time frame on the order of the blanking window length. Thus, multiple strong radars and extended postcursor multipath components are not expected to be a serious problem.

Nevertheless, it is difficult to judge from the above results whether decreasing β is truly resulting in more aggressive blanking. For confirmation, we computed the actual percentage of samples blanked, derived in this case from the change in spectral baseline (noise power spectral density) with changing β. The result is shown in Figure 10. Note that the fraction of samples blanked does in fact increase with decreasing β, confirming that the APB is functioning correctly despite the odd behavior of the max-hold spectra.

Note: References cited below are available via the ESL-IIP document server at http://esl.eng.ohio-state.edu/rfse/iip/docserv.html. This site is password protected – please e-mail ellingson.1@osu.edu for access.

References

[1] J.T. Johnson and S.W. Ellingson, "A Digital Receiver with Interference Suppression for Microwave Radiometry" (Original proposal to the NASA Instrument Incubator Program), The Ohio State University ElectroScience Laboratory IIP Memo 1.

[2] S.W. Ellingson, "A Design Concept for the IIP Radiometer," The Ohio State University ElectroScience Laboratory IIP Memo 2, Jan 11, 2002.

[3] S.W. Ellingson, "Design Concept for the IIP Radiometer RFI Processor," The Ohio State University ElectroScience Laboratory IIP Memo 4, Jan 23, 2002.

[4] S.W. Ellingson, "Functional Design of the Asynchronous Pulse Blanker (Rev. 1)," The Ohio State University ElectroScience Laboratory IIP Memo 14, May 1, 2002.

[5] S.W. Ellingson, "Preliminary RFI Survey for IIP", The Ohio State University ElectroScience Laboratory IIP Memo 21, June 11, 2002.

[6] S.W. Ellingson, "Front End Version 1 Design", The Ohio State University ElectroScience Laboratory IIP Memo 7, February 22, 2002.

[7] G.A. Hampson, "Implementation Results of the Digital IF Processor", The Ohio State University ElectroScience Laboratory IIP Memo 19, May 15, 2002.

[8] G.A. Hampson, "A 256K @ 32-bit Capture Card for the IIP Radiometer", The Ohio State University ElectroScience Laboratory IIP Memo 17, May 10, 2002.

[9] Grant A. Hampson, "Implementation of the Asynchronous Pulse Blanker," The Ohio State University ElectroScience Laboratory IIP Memo 22, Jun 26, 2002.

[10] Grant A. Hampson, “Implementation of a Single FFT Processor,” The Ohio State University ElectroScience Laboratory IIP Memo 25, Jun 23, 2002.

[11] S. W. Ellingson and Grant A. Hampson, “On-Air Test of the IIP Receiver Using Observations of an ATC Radar,” The Ohio State University ElectroScience Laboratory IIP Memo 24, Jun 29, 2002.

[12] S.W. Ellingson, “Analysis and Mitigation of Radar at the RPA,” informal report, January 20, 2002, http://esl.eng.ohio-state.edu/rfse/downloads/rparadar.pdf, also available on the IIP document server.